

a result of lower wind stress since the LIA. The absence of the "Suess effect" (the lowering of  $\Delta^{14}\text{C}$  values from the late 19th century as fossil fuel burning released  $^{14}\text{C}$ -free  $\text{CO}_2$ ) in these records is interpreted as a long-term change in ocean circulation within the southwestern Pacific since the late 1800s (38). Rising  $\Delta^{14}\text{C}$  values since the 1880s indicate a greater influx of younger surface waters, and this reduced oceanic "reservoir effect" overrides the anticipated Suess effect (Fig. 3F). We interpret this shift as a weakening of the wind-driven SEC since the late 19th century, which reduced the transport of upwelled equatorial  $^{14}\text{C}$ -depleted water to the GBR corals.

Our SSTa reconstructions suggest that a stronger latitudinal temperature gradient, relative to the present, may have prevailed during the LIA. General circulation model experiments (9) indicate that the global climate responds to an exaggerated latitudinal temperature difference by intensifying the large-scale atmospheric dynamics of the Hadley circulation cells in order to maintain thermal balance. During the LIA, if warm tropical Pacific SSTs encouraged evaporation (as implied by the coral  $\delta^{18}\text{O}$  records) and a stronger Hadley circulation dried the subtropics, then global average water vapor should have increased. A critical question is where that moisture was transported. Generally, snow cover increases with a strong latitudinal temperature gradient, in part because of cooler high-latitude conditions, but also as a result of a greater atmospheric connection between the tropics and extratropics (10). Our results imply that the tropical oceans may have played an important role in driving the LIA glacial expansion during the repeated advances between 1600 and 1860 (1). Cooling and abrupt freshening of the tropical southwestern Pacific coincided with the weakening of atmospheric circulation at the end of the LIA, when glaciers worldwide began to retreat.

References and Notes

1. J. M. Grove, *The Little Ice Age* (Methuen, London, 1988).
2. T. J. Crowley, G. R. North, *Paleoclimatology* (Oxford Univ. Press, New York, 1991).
3. H. H. Lamb, *Climate, History and the Modern World* (Routledge, London, ed. 2, 1995).
4. R. S. Bradley, P. D. Jones, *The Holocene* **3**, 367 (1993).
5. K. J. Kreutz et al., *Science* **277**, 1294 (1997).
6. L. G. Thompson, E. Mosley-Thompson, W. Dansgaard, P. M. Grootes, *Science* **234**, 361 (1986).
7. P. D. Jones, K. R. Briffa, T. P. Barnett, S. F. B. Tett, *The Holocene* **8**, 455 (1998).
8. P. D. Jones, T. J. Osborn, K. R. Briffa, *Science* **292**, 662 (2001).
9. D. Rind, *J. Geophys. Res.* **103**, 5943 (1998).
10. ———, *Quat. Sci. Rev.* **19**, 381 (2000).
11. See supplemental material on Science Online at [www.sciencemag.org/cgi/content/full/295/5559/1511/DC1](http://www.sciencemag.org/cgi/content/full/295/5559/1511/DC1).
12. M. T. McCulloch, M. K. Gagan, G. E. Mortimer, A. R. Chivas, P. J. Isdale, *Geochim. Cosmochim. Acta* **58**, 2747 (1994).
13. M. K. Gagan et al., *Science* **279**, 1014 (1998).
14. E. J. Hendy, M. K. Gagan, J. M. Lough, in preparation.
15. Sr/Ca and U/Ca were determined by isotope dilution

and analyzed by thermal ionization mass spectrometry and solution inductively coupled plasma mass spectrometry, respectively. For methodological details, see (17).

16. The composite reconstructions are the average of all records, after normalization relative to the longest continuous record (HAV-01B). The  $\delta^{18}\text{O}$  composite is based on eight cores; the Sr/Ca and U/Ca composites are constructed from seven (PAN08B excluded). Error bounds were calculated using 95% confidence intervals for each 5-year period. Periods of higher U/Ca variability coincide with die-offs in two of the cores in 1782–1785 and 1817. Data are available at [www.ngdr.noaa.gov/paleo/pubs/hendy2002](http://www.ngdr.noaa.gov/paleo/pubs/hendy2002).
17. C. Alibert, M. T. McCulloch, *Paleoceanography* **12**, 345 (1997).
18. G. R. Min et al., *Geochim. Cosmochim. Acta* **59**, 2025 (1995).
19. N. A. Rayner, E. B. Horton, D. E. Parker, C. K. Folland, K. B. Hackett, *Version 2.2 of the Global Sea-Ice and Sea Surface Temperature Data Set, 1903–1994* (Hadley Centre for Climate Prediction and Research, Meteorological Office, Bracknell, Berkshire, UK, 1996).
20. M. Bottomley, C. K. Folland, J. Hsiung, R. E. Newell, D. E. Parker, *Global Ocean Surface Temperature Atlas "GOSTA"* (U.K. Meteorological Office, Her Majesty's Stationary Office, London, 1990).
21. B. K. Linsley, G. M. Wellington, D. P. Schrag, *Science* **290**, 1145 (2000).
22. K. R. Briffa, P. D. Jones, F. H. Schweingruber, T. J. Osborn, *Nature* **393**, 450 (1998).
23. M. E. Mann, R. S. Bradley, M. K. Hughes, *Nature* **392**, 779 (1998).
24. T. J. Crowley, *Science* **289**, 270 (2000).
25. P. K. Swart, M. L. Coleman, *Nature* **283**, 557 (1980).
26. The  $\delta^{18}\text{O}$  residual is calculated as

$$\Delta\delta^{18}\text{O} = \partial\delta^{18}\text{O}/\partial T(T_{\delta^{18}\text{O}} - T_{\text{Sr/Ca}})$$

where the temperature-dependent function,  $\partial\delta^{18}\text{O}/\partial T$ , is  $-0.18/^\circ\text{C}$  for *Porites* sp. (13).

27. E. R. M. Druffel, S. Griffin, *J. Geophys. Res.* **98**, 20 (1993).
28. T. M. Quinn et al., *Paleoceanography* **13**, 412 (1998).
29. T. M. Quinn, F. W. Taylor, T. J. Crowley, *Quat. Sci. Rev.* **12**, 407 (1993).
30. M. N. Evans, A. Kaplan, M. A. Cane, *Paleoceanography* **15**, 551 (2000).
31. T. J. Crowley, T. M. Quinn, W. T. Hyde, *Paleoceanography* **14**, 605 (1999).
32. B. K. Linsley, R. B. Dunbar, G. M. Wellington, D. A. Mucciarone, *J. Geophys. Res.* **99**, 9977 (1994).
33. E. Wolanski, *Physical Oceanographic Processes of the Great Barrier Reef* (CRC Press, Boca Raton, FL, 1994).
34. J. M. Lough, *Int. J. Clim.* **17**, 55 (1997).
35. P. J. Isdale, B. J. Stewart, K. S. Tickle, J. M. Lough, *The Holocene* **8**, 1 (1998).
36. T. Delcroix, C. Henin, V. Porte, P. Arkin, *Deep-Sea Res.* **43**, 1123 (1996).
37. S. Sokolov, S. Rintoul, *J. Mar. Res.* **58**, 223 (2000).
38. E. R. M. Druffel, S. Griffin, *J. Geophys. Res.* **104**, 23607 (1999).
39. M. Stuiver, G. W. Pearson, T. F. Braziunas, *Radiocarbon* **28**, 980 (1986).
40. We thank L. Kinsley, H. Scott-Gagan, and J. Cali for analytical assistance; S. Fallon and G. Mortimer for the U/Ca method development; B. Parker and M. Devereux for assistance with the corals; and J. Chappell, C. Hendy, G. Meyers, and two anonymous reviewers for valuable comments on the manuscript. E.J.H. was supported by an Australian Postgraduate Award.

2 November 2001; accepted 22 January 2002

## Microbial Activity at Gigapascal Pressures

Anurag Sharma,\* James H. Scott,\* George D. Cody, Marilyn L. Fogel, Robert M. Hazen, Russell J. Hemley, Wesley T. Huntress

We observed physiological and metabolic activity of *Shewanella oneidensis* strain MR1 and *Escherichia coli* strain MG1655 at pressures of 68 to 1680 megapascals (MPa) in diamond anvil cells. We measured biological formate oxidation at high pressures (68 to 1060 MPa). At pressures of 1200 to 1600 MPa, living bacteria resided in fluid inclusions in ice-VI crystals and continued to be viable upon subsequent release to ambient pressures (0.1 MPa). Evidence of microbial viability and activity at these extreme pressures expands by an order of magnitude the range of conditions representing the habitable zone in the solar system.

Microbial communities adapt to a wide range of pressures, temperatures, salinities, pH, and oxidation states. Although the chemical and physical conditions in these extreme environments are reasonably well constrained, the consequence of these physical parameters on the physiology of microbial communities is not well understood. Significant attention has been focused on the effects of high and low temper-

ature on physiology (1, 2). There is some evidence that elevated pressure may also manifest interesting effects on cellular physiology (3, 4). For example, recent studies report that elevated pressure may lead to enzyme inactivation, compromise cell-membrane integrity, and suppress protein interactions with various substrates (3–6). Whereas the cumulative impact of these pressure-induced effects on microbial metabolism and physiology is an inhibition in growth rate and cellular division in microorganisms (7–9), exactly how these factors affect intact cells is not well understood (4, 10).

Numerous high-pressure studies have been conducted on biological systems; however, these have been either on individual biomol-

Geophysical Laboratory, Carnegie Institution of Washington, 5251 Broad Branch Road, N.W., Washington, DC 20015, USA.

\*To whom correspondence should be addressed. E-mail: [sharma@gl.ciw.edu](mailto:sharma@gl.ciw.edu) (A.S.); [j.scott@gl.ciw.edu](mailto:j.scott@gl.ciw.edu) (J.H.S.)

REPORTS

ecules or “indirect” measurements of cellular growth. In most instances, biological techniques for high-pressure studies (>200 MPa or >2 kbar) do not allow for in situ measurements and observations. Typical experimental designs for high-pressure studies extract samples for subsequent analysis at ambient pressure (4, 11). It would be useful to directly examine the effects of pressure on microbial viability to understand physiological responses and cellular biochemistry (10). Here, we adapted diamond anvil cells (12) to explore the effects of high pressure on microbial life.

We used the rate of microbial formate oxidation as a probe of metabolic viability. The utilization of formate by microorganisms is a fundamental metabolic process in anaerobic environments (13) that can be easily monitored via molecular spectroscopy. We monitored in situ microbial formate oxidation for *Shewanella*

*oneidensis* MR1 (12) to pressures of 1060 MPa, at room temperature (25°C), using Raman spectroscopy (12) in diamond anvil cells (Fig. 1). The Raman data revealed rapid oxidation of formate determined from the reduction in the peak height of C-H vibration mode (14) (Fig. 1). Microscopic observations to pressures of 1060 MPa confirmed continued cell viability (intact and motile) over a duration of more than 30 days. As anticipated, formate oxidation rates were significantly reduced upon the addition of sodium cyanide (0.2 M). Cyanide acts as an inhibitor of respiration by acting in competition as an alternate electron acceptor. This result indicates that the oxidation of formate is coupled to biological respiration. Experiments with heat-inactivated MR1 cells, inactivated at 50°C for ~1 hour until lysis was observed, did not exhibit any detectable chemical changes (Fig. 2). Both cell-free and dead cell controls indicate

that formate oxidation was exclusively a result of biological activity. The decrease in the formate oxidation rates with increasing pressure in living cells, as indicated from the Raman data (Fig. 2), may simply reflect a decrease in the cell numbers (15).

There are studies from Antarctic ice that point to it as a viable ecosystem even when the availability of liquid water is limited due to solidification (16–18). We have extended these experiments to pressures where ice-VI becomes stable and explored how the pressure-sensitive bacteria (4, 19), *Shewanella* MR1 and *Escherichia coli*, respond to this change of state, in a nutrient-rich medium (20). Optical observations at pressures ranging from 40 to 1200 MPa, lower than ice-VI formation (21), detect a gradual decrease in cell motility, an increase in cellular adhesion to surfaces, decrease in cell numbers and reduction in metabolic activity (Fig. 2). Furthermore, methylene blue, when added as an electron acceptor to test for respiration at elevated pressures, remained reduced throughout the experiment, indicating that bacterial respiration continued at elevated pressures (22). At ~1250 MPa, the formation of ice-VI was instantaneous. Initially, mosaics of ice-VI crystals were observed separated by thin “veins” of organic-rich fluid containing the bacteria (Fig. 3). However, over time the ice melted partially along the interstitial veins and developed numerous organic-rich fluid inclusions containing microbial clusters (Fig. 3) [Web movie 1 (12)]. These textural changes in the ice, observed to pressures of 1600 MPa, might either be the consequence of the phase separation associated with the formation of ice in any organic-rich medium, or the result of the microorganisms protecting ice-sensitive cellular components (23, 24). Upon subsequent lowering of pressure to melt the ice, cell survival and viability at the higher pressures were determined by direct cell counts (Fig. 2) on both *E. coli* [ranging from 10<sup>6</sup> cells (at 0 hours) to 10<sup>4</sup> cells (after 30 hours)] and *Shewanella* MR1 [ranging

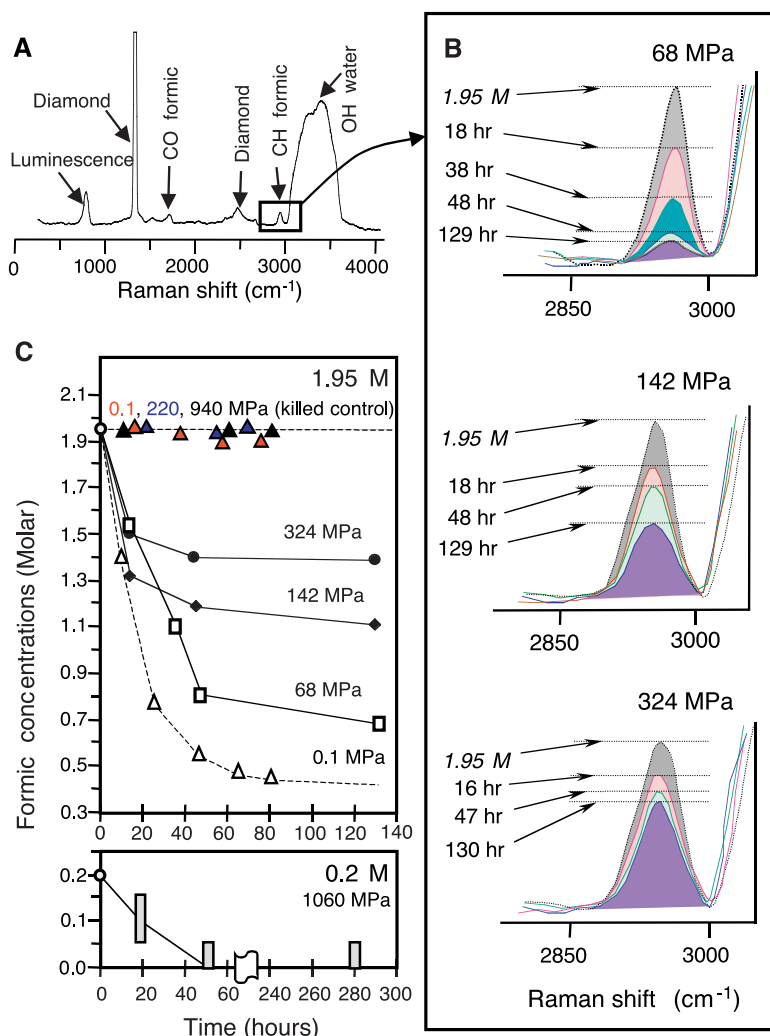


**Fig. 1.** Raman spectra of the formic-biological system (A) shown with the vibration peaks of formic and diamond anvils used in this study. The outlined boxed region is shown at higher resolution (B) to quantify the successive decrease in the peak intensity of the C-H stretch of formic acid at pressures of 68, 142, and 324 MPa. The equivalent formate concentrations (C), corresponding to each peak height change, are based on comparisons with a known calibration curve. All experiments were performed at 25°C, with diamond anvil cells (32) with gold-lined sample chambers (12). Pressures were estimated using Raman shifts in quartz used as an internal calibrant (14).

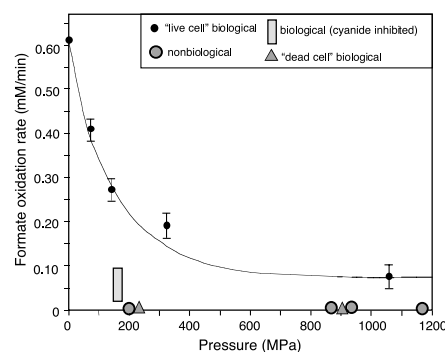


**Fig. 2.** Shown are formate oxidation rates for experiments at high pressures for the first 48 hours. Whereas biological formate oxidation rates exhibit an inversely exponential relationship with pressure, the cyanide-inhibited system shows a lower formate oxidation rate.

## REPORTS

from  $3 \times 10^6$  cells (at 0 hours) to  $10^4$  cells (after 30 hours) (20)] (Fig. 3). Distinct changes in cellular morphology were also observed, including a significant increase in cell size and polar invaginations, both clear indications of arrested cellular division (25, 26). Upon a subsequent increase of pressure to 1680 MPa, the veins of organic-rich fluids developed a "stringy" texture as well as an increase in fluorescence background in Raman spectra. This could be an indication of cellular lysis, because no live cells were observed upon return to ambient pressure.

Adaptability of *Shewanella* MR1 as well as *E. coli* in these experiments indicates that microorganisms can continue to metabolize substrate at pressures far beyond those previously reported in the literature (3, 4, 10). Although an evolutionary component to the adaptation of microbial communities to temperature and salinity is well known (27), whether there might

be any evolutionary component for pressure adaptation is still in question. *Shewanella* MR1 belongs to a genus that contains a number of piezophiles; however, *E. coli* clearly does not. Despite this, there is evidence that exposure of *E. coli* to pressures up to 800 MPa selects a population of cells less sensitive to pressure inactivation (19). Furthermore, it is well known that the increase in pressure tolerance is also associated with heat tolerance (19). Our observations on pressure-sensitive bacteria may indicate that piezo-tolerance of these bacteria could be a protective mechanism in response to stress (4, 28, 29). Whether this is a short-term or an evolutionary adaptation remains unanswered.

These results imply that pressure may not be a significant impediment to life. The maximum pressure explored in this work is equivalent to a depth of  $\sim 50$  km below Earth's crust, or  $\sim 160$  km in a hypothetical ocean. The pressures encountered at the depths of

thick ice caps and deep crustal subsurface may not be a limiting factor for the existence of life. This suggests that deep (water/ice) layers of Europa, Callisto, or Ganymede, subduction zones on Earth, and the polar ice caps of Mars might provide viable settings for life unhindered by the high pressures (30, 31).

### References and Notes

1. T. D. Brock, *Science* **158**, 1012 (1967).
2. J. W. Deming, J. A. Baross, *Geochim. Cosmochim. Acta* **57**, 3219 (1993).
3. D. H. Bartlett, *Sci. Progress* **76**, 479 (1992).
4. F. Abe, C. Kato, K. Horikoshi, *Trends Microbiol.* **7**, 447 (1999).
5. C. A. Royer, *High Pressure Res.* **19**, 213 (2000).
6. Y. Yano, A. Nakayama, K. Ishihara, H. Saito, *Appl. Environ. Microbiol.* **64**, 479 (1998).
7. C. E. Zobell, in *Ken Sugawara Festival Volume*, Y. Miyake, T. Koyoma, Eds. (Maruzen, Tokyo, 1964), pp. 83–116.
8. C. O. Wirsén, S. J. Molyneux, *Appl. Environ. Microbiol.* **65**, 5314 (1999).
9. C. E. Zobell, *Science* **115**, 907 (1952).
10. F. Abe, K. Horikoshi, *Trends Biotechnol.* **19**, 102 (2001).
11. A. A. Yayanos, in *Extremophiles*, K. Horikoshi, W. D. Grant, Eds. (Wiley, New York, 1998), chap. 3.
12. Web note 1. Supplemental material is available on Science online at [www.sciencemag.org/cgi/content/full/295/5559/1514/DC1](http://www.sciencemag.org/cgi/content/full/295/5559/1514/DC1).
13. J. G. Ferry, *FEMS Microbiol. Rev.* **7**, 377 (1990).
14. Web note 3 (12).
15. Web note 4 (12).
16. P. B. Price, *Proc. Natl. Acad. Sci. U.S.A.* **97**, 1247 (2000).
17. J. C. Priscu et al., *Science* **286**, 2141 (1999).
18. D. M. Karl et al., *Science* **286**, 2144 (1999).
19. K. J. A. Hauben et al., *Appl. Environ. Microbiol.* **63**, 945 (1997).
20. Web note 2 (12).
21. In pure H<sub>2</sub>O system, ice-VI forms at  $\sim 900$  MPa [H. T. Haselton Jr., I. M. Chou, A. H. Shen, W. A. Bassett, *Am. Mineral.* **80**, 1302 (1995)]. However, the presence of organics in solution changes the chemical potential of H<sub>2</sub>O resulting in freezing point shift to higher pressures.
22. Methylene blue (0.05 mM) was used to indicate metabolic activity. Under reduced conditions the dye changes color from blue-violet (oxidized) to colorless (reduced) [K. M. Jones, in *Data for Biochemical Research*, R. M. C. Dawson, D. C. Elliott, W. H. Elliott, K. M. Jones, Eds. (Oxford Univ. Press, London, 1969), pp. 436–455], because it is used as an alternate electron acceptor by *Shewanella* MR1 [J. H. Scott, K. H. Nealson, *J. Bacteriol.* **176**, 3408 (1994)] and *E. coli* [H. G. Enoch, R. L. Lester, *J. Biol. Chem.* **250**, 6693 (1975)]. Furthermore, methylene blue in its reduced form during anaerobiosis is an indication of flavoprotein activity in the bacteria.
23. J. F. Carpenter, T. N. Hansen, *Proc. Natl. Acad. Sci. U.S.A.* **89**, 8953 (1992).
24. J. C. Priscu et al., *Science* **280**, 2095 (1998).
25. C. E. Zobell, A. B. Cobet, *J. Bacteriol.* **84**, 1228 (1962).
26. ———, *J. Bacteriol.* **87**, 710 (1963).
27. C. R. Woese, O. Kandler, M. L. Wheelis, *Proc. Natl. Acad. Sci. U.S.A.* **87**, 4576 (1987).
28. T. J. Welch, A. Farewell, F. C. Neidhardt, D. H. Bartlett, *J. Bacteriol.* **175**, 7170 (1993).
29. K. Liberek, T. P. Galitski, M. Zyllicz, C. Georgopoulos, *Proc. Natl. Acad. Sci. U.S.A.* **89**, 3516 (1992).
30. C. F. Chyba, C. B. Phillips, *Proc. Natl. Acad. Sci. U.S.A.* **98**, 801 (2001).
31. M. H. Carr et al., *Nature* **391**, 363 (2000).
32. W. A. Bassett, A. H. Shen, M. Bucknum, I. M. Chou, *Rev. Sci. Instrum.* **64**, 2340 (1993).
33. We thank H. S. Yoder Jr., K. H. Nealson, D. H. Bartlett, and W. A. Bassett for insightful discussions. This study was supported by Carnegie Institution of Washington and NASA Astrobiology Institute.

13 November 2001; accepted 23 January 2002

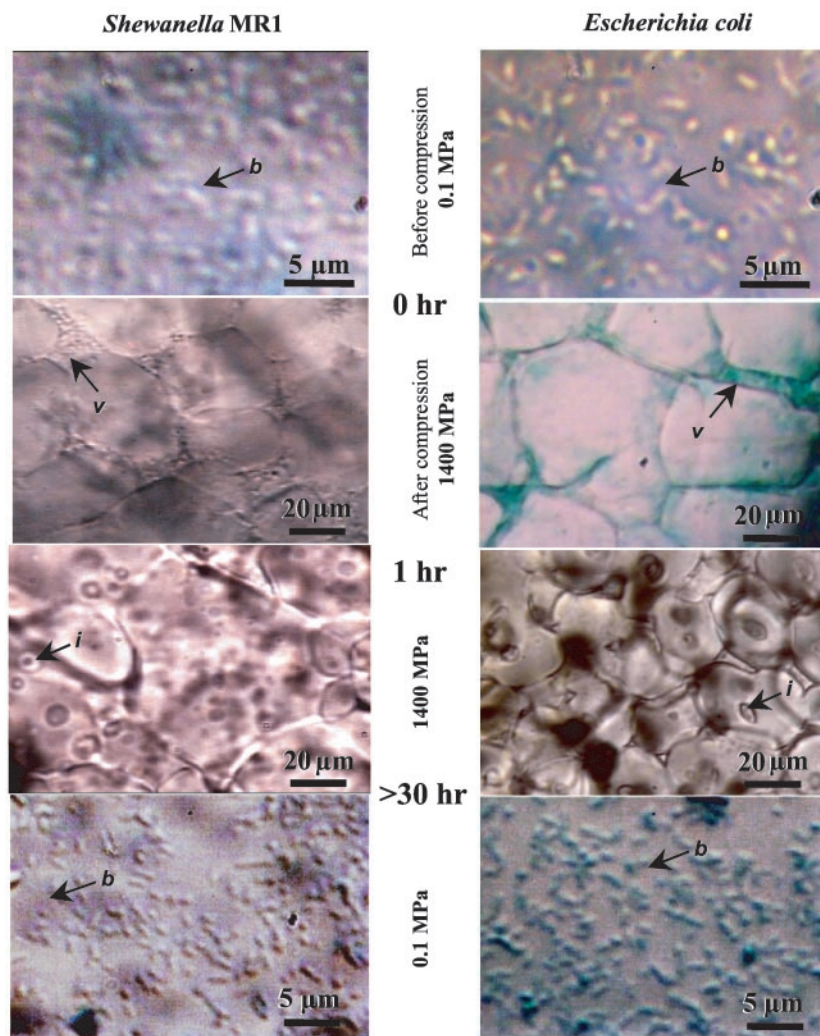


**Fig. 3.** Microbial activity and viability in ice-VI. Upon ice nucleation (0 hours, 1400 MPa), organic fluid veins (*v*) filled with bacteria (*Shewanella* MR1 on the left, *E. coli* stained with methylene blue on the right) appear. After  $\sim 1$  hour, textural changes in the ice occur, defined by the formation of organic-rich inclusions (*i*) containing motile bacteria [Web movie 2 (12)]. Viable (methylene blue in solution remains colorless indicating respiration) and countable bacteria (*b*) were observed upon subsequent lowering of pressure [Web movie 3 (12)].